Chapter 6

Multiojective Calibration: More Empirical Evidence

In Chapter 5 we have shown that the consistency hypothesis stated by Björk [9, 10], implies that the discount bond curve has to be determined at the same time as the parameters of the model. Angelini and Herzel [1, 2], originally proposed the use of a optimization program related to the mentioned daily calibrations, which is compatible with this joint estimation. The milestone of this methodology is the use of an objective function based on an error measure for just the portfolio of caps. Then, the theoretical prices for the caps along the minimization of this measure can be calculated at the same time that the discount bond curve is fitted. This is an efficient method because consistent families of discount bond curves have good analytical properties under the Gaussian hypothesis, i.e. deterministic *forward* volatility.

In last chapter, we have also provided an extension of the above strategy which involves a multi-objective framework. As a direct consequence, the objective function above-mentioned, is subtituted by a *scalarized* form of the intrinsic bi-objective problem. Now, the error measure for the discount bonds is evaluated in each iteration and could even dominate the joint optimization problem. To this scope, we construct this *scalarized* form using a convex combination of both the cap and the bond error measures, by means of a set of restricted weights. As a matter of fact, this approach is richer in possible outcomes.

6.1 Introduction

Given the theoretical tools we have developed in the previous chapters, we want to analyze further empirical results which support the use of consistent families and the multi-objective calibration techniques.

To this end, we extend such analysis to a particular humped volatility HJM model, proposed by Ritchen and Chuang [39] and Mercurio and Moraleda [34], independently. We have chosen this model because it is quite popular and analytically treatable. In particular, it provides closed formulas for Europeans interest-rate options. Moreover, it is a one-factor Gaussian model that seems to be more capable than the Hull-White model for reproducing large humps in the implied cap volatility curve.

We perform our study by calibrating this model, first by using simulated data and second by focusing on market a data set composed by US discount bonds and at-the-money flat cap volatilities quotes in two different periods, as shown by the Figure 6.1.

With regard to the real market data, the first scenario depicts a market situation where the implied cap volatility curves have a large long-term humped shape and the term structure of interest rates is closer to be flat. On the other hand, the second scenario has periodically resurfaced in the market and may be considered more typical. In this situation the peak of the hump is at about the two year point. Moreover, the TSIR is not monotonic increasing nor flat, being initially-inverted with a local minimum at short-term maturities.

This rest of this chapter is organized as follows[1]. In Section 6.2 we give a brief overview of the model we want to consider and later we discuss how to construct consistent families with such a model. Section 6.3 is devoted to empirical results, first comparing the consistent calibration with the non-consistent approach by means of simulated data, then presenting the results of the fitting of the different methods with market data. In the last section we give some final conclusions and remarks.

[1]This chapter is based on [19, 21].

Figure 6.1: Market TSIR and TSV data in the two different market scenarios.

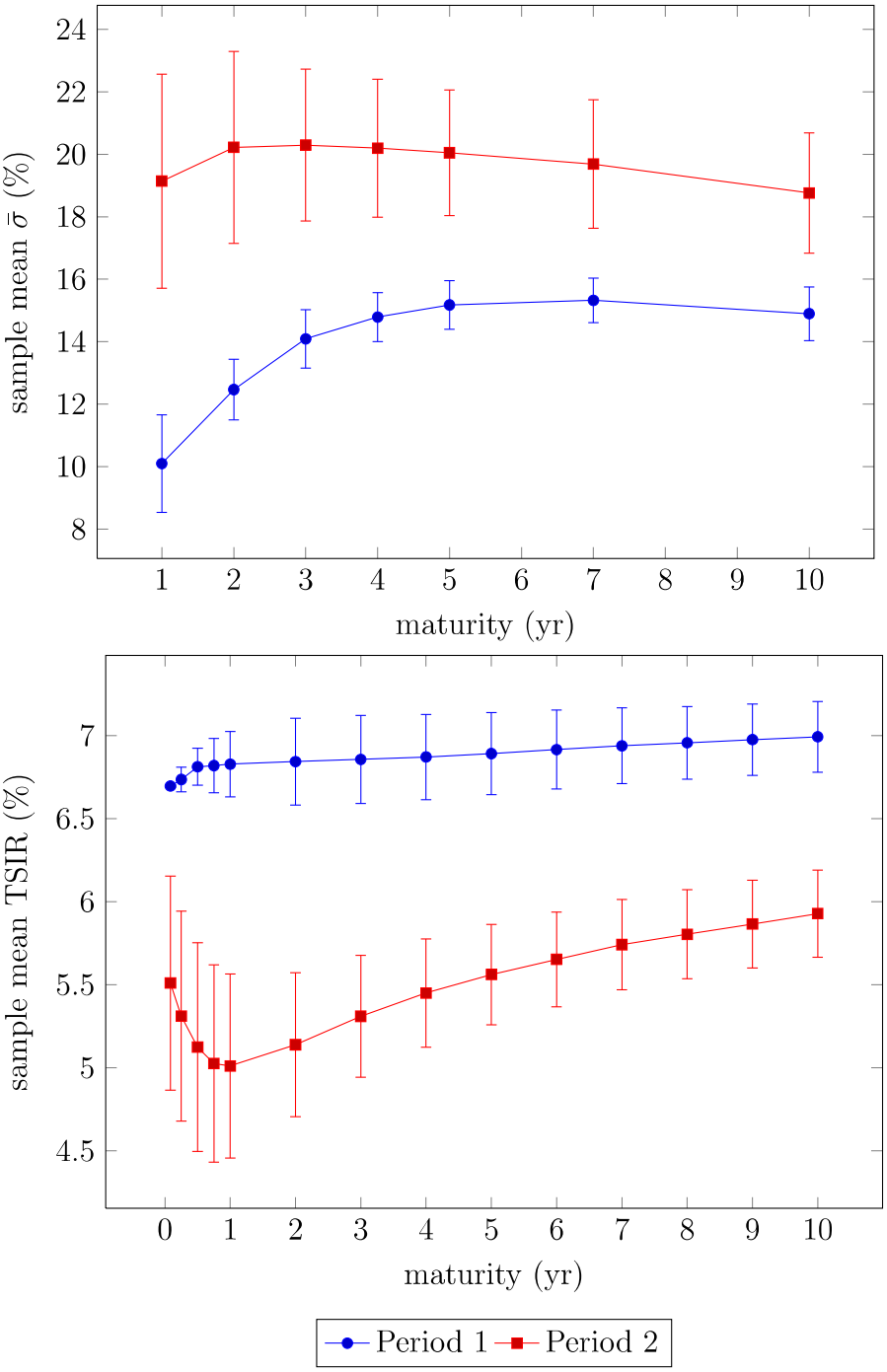

6.2 Consistent Curves with The Model

Our work is devoted to the one-dimensional Gaussian HJM humped volatility model of the form:

$$df_t(x) = \{\dots\}\, dt + (\alpha + \beta x)\, e^{-ax}\, dW_t. \tag{6.1}$$

Thus, the forward rate volatility function $\sigma(x)$ is deterministic depending only on time to maturity. Note that $\sigma(x)$ is a QE function that admits the matrix representation (5.19). Therefore, $\sigma(x)$ may be rewritten as

$$\begin{aligned} \sigma(x) &= ce^{Ax}b, \text{ where} \\ c &= [\alpha \quad \beta - a\alpha], \\ A &= \begin{bmatrix} 0 & -a^2 \\ 1 & -2a \end{bmatrix}, \\ b &= \begin{bmatrix} 1 \\ 0 \end{bmatrix}. \end{aligned} \tag{6.2}$$

For this model, the forward rate decomposition $f_t(x) = \delta_t(x) + q_t(x)$, as seen before in Sect. 5.3, eqs. (5.21)–(5.22), has the corresponding q_t-process dynamics:

$$dZ_t = AZ_t\, dt + b\, dW_t, \quad Z_0 = 0, \tag{6.3}$$

$$q_t(x) = C(x)Z_t, \tag{6.4}$$

with A, b as in (6.2) and $C(x) = ce^{Ax}$. Therefore, the analytical expression of the forward rate curve for the model is given by

$$f_t(x) = f^o(x+t) + \frac{1}{2}\left[S^2(t+x) - S^2(x)\right] + C(x)Z_t, \tag{6.5}$$

being $S(x) = \int_0^x \sigma(u)\, du$. After some algebraic manipulations like using the explicit expansion for the stochastic term $C(x)Z_t$

$$ce^{Ax}\begin{bmatrix} Z_t^1 \\ Z_t^2 \end{bmatrix} = e^{-ax}\,[\alpha \;\; \beta - a\alpha]\begin{bmatrix} 1+ax & -a^2x \\ x & 1-ax \end{bmatrix}\begin{bmatrix} Z_t^1 \\ Z_t^2 \end{bmatrix}$$

$$= e^{-ax}\left(\alpha Z_t^1 - a\alpha Z_t^2 + \beta Z_t^2\right) + xe^{-ax}\left(\beta Z_t^1 - a\beta Z_t^2\right),$$

and expanding the deterministic term $\frac{1}{2}\left[S^2(t+x) - S^2(x)\right]$ which is of the form

$$g_1(t)e^{-2ax} + g_2(t)xe^{-2ax} + g_3(t)x^2e^{-2ax} + h_1(t)e^{-ax} + h_2(t)xe^{-2ax},$$

(6.5) may be written as

$$\begin{aligned} f_t(x) = f^o(x+t) + g_1(t)e^{-2ax} + g_2(t)xe^{-2ax} + g_3(t)x^2e^{-2ax} + \\ \left(h_1(t) + \alpha Z_t^1 - a\alpha Z_t^2 + \beta Z_t^2\right)e^{-ax} + \left(h_2(t) + \beta Z_t^1 - a\beta Z_t^2\right)xe^{-ax}. \end{aligned} \tag{6.6}$$

Note that this formula, as its corresponding counterpart in previous chapter (5.28), is relevant for consistency, because it shows which curves the model produces for a given initial curve $f^o(x)$.

6.2.1 The Minimal Consistent family

Proposition 11 *The family*

$$G_{HMC}(z,x) = (z_1 + z_2x)e^{-ax} + (z_3 + z_4x + z_5x^2)e^{-2ax}, \tag{6.7}$$

is the minimal dimension consistent family with the model characterized by deterministic volatility $\sigma(x) = (\alpha + \beta x)e^{-ax}$.

Proof. From (6.6) we see that a family which is invariant under time translation is consistent with the model if and only if it contains the linear space $\{e^{-ax}, xe^{-ax}, e^{-2ax}, xe^{-2ax}, x^2e^{-2ax}\}$. □

Similar results as discussed along the lines of Sect. 5.2.1 will turn up over and over again, so we list some concluding remarks which the reader may immediately derive.

Lemma 3 *The following hold for the humped volatility Heath-Jarrow-Morton model characterized by* $\sigma(x) = (\alpha + \beta x)e^{-ax}$.

- *The NS*

  $$G_{NS}(z,x) = z_1 + z_2e^{-z_4x} + z_3xe^{-z_4x},$$

  is not consistent with this model.

- *The family*

  $$G_{HMC}(z,x) = (z_1 + z_2x)e^{-ax} + (z_3 + z_4x + z_5x^2)e^{-2ax},$$

it is the lowest dimension family consistent with the model (hereafter HMC).

- *The family*

$$G_{ANS+}(z,x) = z_1 + z_2 e^{-ax} + z_3 x e^{-ax} + (z_4 + z_5 x + z_6 x^2) e^{-2ax},$$

is the simplest adjustment based on restricted NS family that allows model consistency (hereafter ANS+).

6.3 Empirical Results

We compare four different estimations of the initial discount bond curve based on NS, HMC, ANS+ and cubic spline interpolation (hereafter SP).

The US data set consists of 126 daily observations divided in two periods: first period covers from 3/7/2000 to 29/09/2000 (64 trading dates) and the second one starts in 4/1/2001 and finish on 30/3/2001 (62 trading dates).

With regard to the market the data set is composed of US discount bond of fourteen maturities (1, 3, 6 and 9 months and from 1 to 10 years) and of implied volatilities of at-the-money interest rate caps with maturities 1, 2, 3, 4, 5, 7 and 10 years. This two windows of data comes from the same database explained before in Chapter 5 being kindly provided by Thomson Reuters Datastream. On the other hand, the simulated data was obtained from 360 extractions of bond and cap prices with identical maturities as its real-market equivalents as produced by the model under study.

Simulations

We simulate the forward rate curves of the humped volatility model at time t when initiliazed from alternative starting curves $f^o(x)$ using (6.6).

Next, we compute the fourteen prices of the set of discount bonds by integrating the forward curve $f_t(x)$ in

$$P(t,x) = e^{-\int_0^x f_t(u)\,du},$$

and the seven prices of the ATM caps by using equations (5.29), (3.13), (3.18), and by working out the integral (3.19) to obtain the model implied volatility

function:

$$\vartheta^2(0, x_{j-1}) = \int_0^{x_{j-1}} \left[\int_{x_{j-1}}^{x_j} (\alpha + \beta(T-t)) e^{-a(T-t)}\, dT \right]^2 dt. \tag{6.8}$$

The fixed model parameters, $\boldsymbol{p_0} = [0.002\ 0.007\ 0.35]^T$, have been taken. This particular choice has similar order of magnitude as the empirical estimations for this model reported by Angelini and Herzel [2]. As alternative starting curves, we choose HMC, ANS+ and NS fitted to the zero coupon bond prices shown in Figure 6.2.

Figure 6.2: Discrete data for initial yield-curve estimation.

Maturity, x	0.083	0.25	1	2	3	4
Discount Bond, $P^o(x)$	0.9962	0.9886	0.9538	0.9069	0.8602	0.8142
Maturity, x	5	6	7	8	9	10
Discount Bond, $P^o(x)$	0.7693	0.7260	0.6843	0.6445	0.6066	0.5706

Starting from the initial fitted curves, which may be denoted with $f^o_{HMC}(x)$, $f^o_{ANS+}(x)$ and $f^o_{NS}(x)$, and according to (6.5), the corresponding three different model evolutions are calibrated to HMC, ANS+ and NS, restricting the palette of the possible Pareto-front approximants produced by the *scalarized* program (5.45), to $\omega_1 = 1$. In order to make calibration results more comparable, Monte Carlo simulations are built in from the identical random sequence $(Z_t^1,\ Z_t^2)$ in all three cases.

Following the expression (6.6), it is easy to observe that there are two consistent families, G_{HMC} and G_{ANS+}, for the first simulation E1, just one, G_{ANS+}, for the second simulation E2, and no one for the last simulation E3.

Figure 6.3 shows main consequences of the theory when the model is the *truth* model. Notice that perfect calibration just occurs, although model parameters are fixed *a priori*, when the used family to perform calibrations is consistent with all the future forward curves generated from initial curve $f^o(x)$. This fact explains, for instance, the bad performance for the NS family even on E3 experiment. Indeed, as may be seen in Figure 6.4, an incorrect discount bond choice selection produces parameter instability and imprecision.

Figure 6.3: Summary statistics for calibration results with simulated data.

		MC	ANS	NS
E1: $f_0(x) = f^o_{HMC}(x)$	$\varepsilon_r(\alpha)$	0	0	0.23
	$\varepsilon_r(\beta)$	0	0	0.13
	$\varepsilon_r(a)$	0	0	$8.7\ 10^{-2}$
	$C_v(\alpha)$	0	0	0.18
	$C_v(\beta)$	0	0	0.14
	$C_v(a)$	0	0	$9.7\ 10^{-2}$
	σ_{LS}	0	0	$1.9\ 10^{-3}$
E2: $f_0(x) = f^o_{ANS+}(x)$	$\varepsilon_r(\alpha)$	0.25	0	0.28
	$\varepsilon_r(\beta)$	0.16	0	0.16
	$\varepsilon_r(a)$	0.12	0	$9.5\ 10^{-2}$
	$C_v(\alpha)$	$3.8\ 10^{-2}$	0	0.117
	$C_v(\beta)$	$3.9\ 10^{-2}$	0	$9.1\ 10^{-2}$
	$C_v(a)$	$3.2\ 10^{-2}$	0	$4.8\ 10^{-2}$
	σ_{LS}	$2.6\ 10^{-4}$	0	$6.7\ 10^{-4}$
E3: $f_0(x) = f^o_{NS}(x)$	$\varepsilon_r(\alpha)$	0.313	$2.7\ 10^{-4}$	0.18
	$\varepsilon_r(\beta)$	0.20	$2.10\ 10^{-4}$	0.10
	$\varepsilon_r(a)$	0.16	$1.6\ 10^{-5}$	$6.7\ 10^{-2}$
	$C_v(\alpha)$	$2.3\ 10^{-2}$	$1.4\ 10^{-4}$	0.17
	$C_v(\beta)$	$2.6\ 10^{-2}$	$1.0\ 10^{-4}$	0.111
	$C_v(a)$	$2.2\ 10^{-2}$	$8.3\ 10^{-5}$	$6.3\ 10^{-2}$
	σ_{LS}	$3.8\ 10^{-4}$	$3.9\ 10^{-9}$	$3.5\ 10^{-4}$

Sample statistics of the calibration on simulated data. Relative errors of the parameters estimates are expressed in absolute value. We set to 0 table entries with value $< 10^3 \cdot$`eps` (variable `eps` $\sim 10^{-16}$ measures MATLAB internal accuracy).

Real Data

The main purpose of this section is to compare the performance of the two different calibration approaches introduce in Chapter 5 along the two different periods of real trading dates described before. Therefore, from now on we will only consider the calibration results obtained with the market data. For simplicity, the consistent calibrations are carried out by means of just the lowest dimension family, the HMC family.

Concerning the real data, calibration with consistent families are carried out by setting the weights palette (ω_1, ω_2), as defined in (5.42), Sect. 5.5. With regard to the consistent calibration, the *scalarized* MOO program (5.45) has also been used. The table on Figure 6.5 exhibits the sample mean of the daily error

Figure 6.4: Daily estimates of parameters a and α for data simulated from the model with $\alpha = 0.002$ and $a = 0.35$ and starting forward curve $f_0(x) = f^o_{ANS}(x)$.

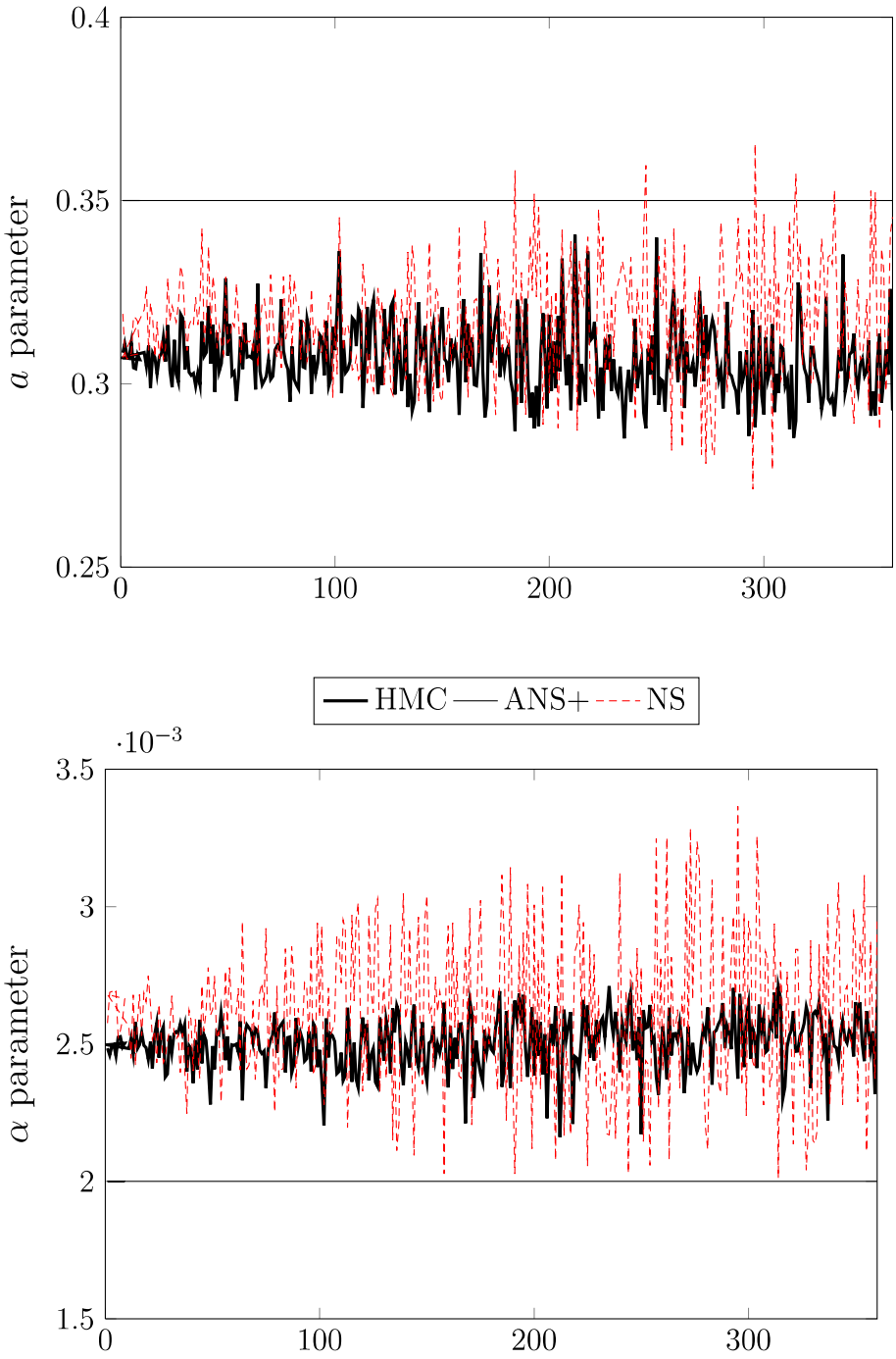

The straight line corresponds to daily calibration results belonging ANS+ family, the irregular black line to the MC family and the dashed red one to the NS family.

fitting measures, namely RPE_C and RPE_B, and the mean and the coefficient of variation of parameter estimates.

Figure 6.5: Summary statistics for calibration results with US data on both periods.

		MC	NS	SP
Period 1	α	0.0093	0.0098	0.01
	β	0.0007	0.0013	0.0008
	a	0.0024	0.0961	0.064
	$C_v(\alpha)$	0.11	0.05	0.05
	$C_v(\beta)$	0.33	0.71	1.30
	$C_v(a)$	0.52	0.54	0.92
	$RPE_C(\%)$	2.2	2.7	2.75
	$RPE_B(\%)$	0.019	0.047	
Period 2	α	0.0087	0.0091	0.0085
	β	0.0041	0.0039	0.0052
	a	0.1469	0.176	0.2129
	$C_v(\alpha)$	0.15	0.1	0.11
	$C_v(\beta)$	0.72	0.38	0.35
	$C_v(a)$	0.96	0.3	0.27
	RPE_C	1.49	1.56	1.36
	RPE_B	0.031	0.043	

On the other hand, Figure 6.7 shows in-sample fitting time series. The HMC family under study report good in-sample fitting results as compared with non-consistent approaches. However, when we look in detail at the Period 2, the families NS and HMC and even the cubic spline based interpolants perform slightly similar with regard to caps calibration. In fact, the non-consistent approach based with cubic spline interpolation, outperforms marginally all the rest. In Figure 6.6, we plot the daily distribution of the weight ω_1 which performs the best calibration for caps in both samples of data. As for the Period 1, we observe that the cap contribution of the scalarized objective is more dominant, because of the reason that when articulating *a posteriori* preferences as we made in previous chapter, the weights closer to the WPO ($\omega_1 = 1$) have the capability to reproduce better daily fits of derivatives. As for the Period 2, the individual objectives, $[l_1\ l_2]^T$ appear to be more cooperative relaxing the performance of the fit results of the implied cap volatility curve major. This fact, may explain the very similar results

provided for all three methods in the second window.

Figure 6.6: Not normalized daily empirical distribution of weights with the best RPE_C for both sample periods as produced by the multi-objective calibration.

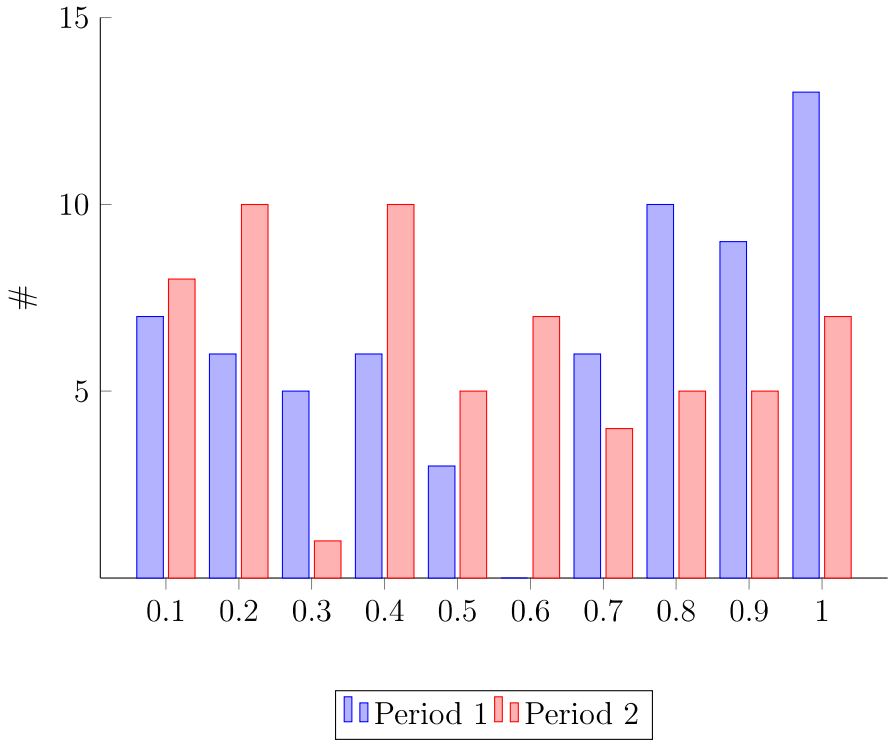

6.4 Conclusions

In this chapter, we analyze two new consistent families of curves (the HMC and ANS+ families) for comparing to another non-consistent approaches like cubic spline interpolation as well as the well-known Nelson and Siegel family. In so doing, we have tried to support and extend to another treatable Gaussian model the empirical findings of Chapter 6.

When using simulated data it is very clear that the consistent families for the E1 ans E2 experiments performs much better than the non-consistent ones. Moreover, Nelson-Siegel family does not work even if it is chosen as the starting yield-curve (recall E3 experiment). These empirical facts constitute a nice demonstration of the theory introduced in Chapter 4, in the sense that even on absence of *model risk* only when consistent families are used, perfect calibration may occur.

Translation of these consequences to real data is less clear, due to *model risk* and quality of data but we can infer the following concluding remarks. In this case, the introduction of a sufficiently rich *consistent families* like HMC which us well motivated theoretically by Björk et al., improves in-sample fitting capabilities on caps on bonds complementing what Angelini and Herzel [1, 2] empirically found with differents sets of data. According to the results reported for the humped volatilty model in this chapter and the Hull-White model in Chapter 5, multi-objective calibration would lead generally to better results in caps calibration as compared to non-extended consistent calibration (originally introduced in [1, 2]) and the more traditional non-consistent methodologies.

Finally, future empirical research on the matter should include multi-factor models for capturing more appropriately the TSIR and TSV observed in the market.

Figure 6.7: In-sample fitting time series for the first period (left) and the second period (right) with real market data.

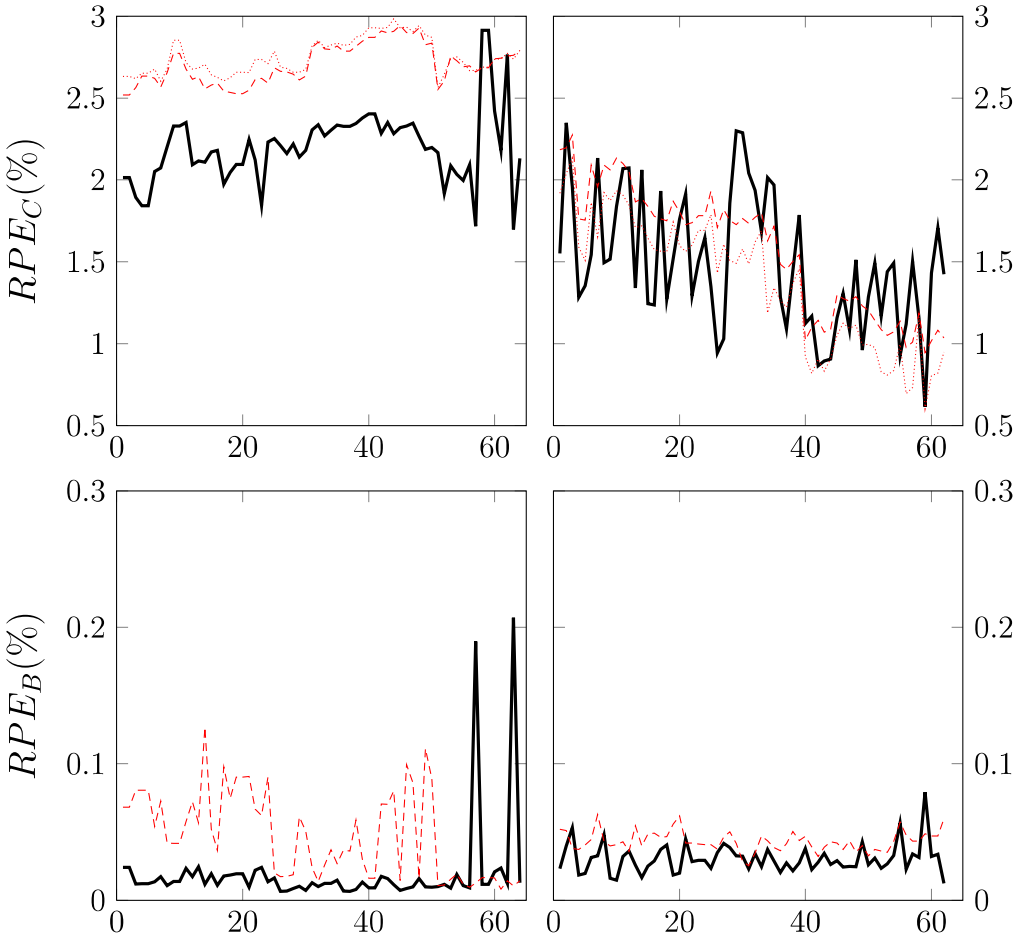

The thick black line corresponds to the minimal consistent family, the dashed red line to the NS family and the dotted one to cubic spline interpolation.